

Proximity effect on the general base catalysed hydrolysis of amide linkage: The role of cationic surfactant, CTABr

SARAT C DASH and ANADI C DASH*

Department of Chemistry, Utkal University, Bhubaneswar 751 004, India
e-mail: acdash1@rediffmail.com

MS received 18 August 2010; accepted 28 February 2011

Abstract. The *bis* phenoxide forms of (1,2)*bis*(2-hydroxybenzamido)ethane(**I**), (1,5)*bis*(2-hydroxybenzamido)3-azapentane(**II**), (1,3)*bis*(2-hydroxybenzamido)propane(**III**), and (1,8)*bis*(2-hydroxybenzamido)3,6-diazaoctane(**IV**) undergo facile hydrolysis of one of the amide groups ($0.02 \leq [\text{OH}^-]_{\text{T}} (\text{mol dm}^{-3}) \leq 0.5$, 10% MeOH (v/v) + H₂O medium) without exhibiting $[\text{OH}^-]$ dependence. The reactivity trend follows **I** ~ **II** >> **III** ~ **IV** with low activation enthalpy $\{25.7 \pm 2.8 \leq \Delta H^\ddagger (\text{kJ mol}^{-1}) \leq 64.8 \pm 7.0\}$. The high negative and comparable values of activation entropy $\{-234 \pm 8 \leq \Delta S^\ddagger (\text{J K}^{-1} \text{mol}^{-1}) \leq -127 \pm 20\}$ are consistent with closely similar, and ordered transition states which can be assembled by favourably oriented phenoxide groups. The solvent kinetic isotope effect for **I**, $k^{\text{H}_2\text{O}}/k^{\text{D}_2\text{O}+\text{H}_2\text{O}} \sim 1$ (20 and 50 volume% D₂O), indicates that proton transfer is not involved as a part of the rate controlling process. The observed slowing down of the rate of this reaction for **I** in the micellar pseudo phase of CTABr also supports the proposed mechanism. Under pre-micellar conditions, however, rate acceleration is observed, a consequence believed to be associated with the capping effect of the hydrophobic tail of the surfactant cation forming the reactive ion-pair, CTA⁺, (I-2H)²⁻ exclusively in the aqueous pseudo phase.

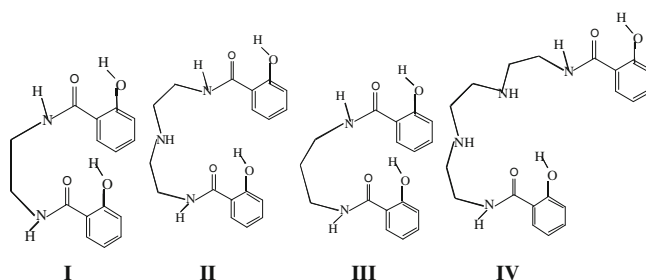
Keywords. 2-Hydroxybenzamides; kinetics; micellar effect.

1. Introduction

The amide moiety is a fundamental unit in biological chemistry. Its remarkable resistance to hydrolysis is a key feature of the stability of complex protein structures. However, the amide unit in a molecule can suffer slow hydrolytic splitting under the catalytic action of acids and bases. Brown *et al.*¹ reviewed this aspect in 1992 and discussed the influence of stereo-electronic effects of the functional groups attached to the amide *N*-site. Subsequent to this Bowden *et al.*² reported the intra molecular catalysis by neighbouring carbonyl group in the alkaline hydrolysis of 2-formyl acetanilide and related amides. In the recent years considerable emphasis has been attached to the polydentate ligands endowed with phenol–amide functionalities. Several transition metal complexes of such ligands have been synthesized, structurally characterized,^{3,4} and their catalytic applications in organic synthesis in limited cases have been demonstrated.^{5,6} We have been working on the solution state kinetics and equilibria involving polydentate phenol–amide ligands and transition metal ions

with a view to understand the mechanism of binary and ternary complex formation and electron transfer processes.⁷ As a part of this program we felt it worthwhile to investigate the kinetics of acid and base hydrolysis of such polydentate amide ligands.

We have chosen (1,2)*bis*(2-hydroxybenzamido)ethane(**I**), (1,5)*bis*(2-hydroxybenzamido)3-azapentane(**II**), (1,3)*bis*(2-hydroxybenzamido)propane(**III**), and (1,8)*bis*(2-hydroxybenzamido)3,6-diazaoctane(**IV**) in order to examine the intramolecular participation of the phenol (phenoxide), if any, on the hydrolysis of the amide function. The relevant literature survey showed to the best of our knowledge that it has not been reported earlier. However, data are available for salicylamide and related systems^{1,8} for comparison.



*For correspondence

2. Experimental

2.1 Materials

The amines, (1,2)diaminoethane, (1,3)diaminopropane, (1,5)diamino 3-azapentane, and (1,8)diamino 3,5-diazaoctane (BDH), methyl salicylate (Siscochem/Merck, India) were used as received. The *bis* (2-hydroxybenzamides) of the multidentate amines (**I–IV**) were synthesized by condensing the respective amines with methyl salicylate in 1:2 mol ratio at 70°C and purified by re-crystallization from 50% (v/v) methanol water mixture.^{9–12} The samples were air dried and stored over silica gel in a desiccator for further drying. The purities of the samples (**I–IV**) were further checked by elemental analyses which were in good agreement with the calculated values. The IR spectra displayed strong band at 1630–1646 cm⁻¹ characteristic of $\nu_{\text{str.}}(\text{C}=\text{O})$ as reported earlier.^{9–11} The UV-Vis spectral data for the samples are as follows: λ_{max} , nm (ϵ , dm³ mol⁻¹ cm⁻¹): 297.0 (6089) [**I**], 298.0 (6971) [**II**], 298.5(6306) [**III**], 298.0 (7925) [**IV**].

Cetyltrimethylammonium bromide (CTABr) (Aldrich, 99%) was used as received. All other chemicals used in the kinetic study were of analytical grade. Methanol was GR grade (Merck, purity 99.8%). Water was doubly distilled, the second distillation being made from alkaline KMnO₄ in an all glass distillation apparatus. All reactions were studied in 10% (v/v) MeOH + H₂O medium unless otherwise mentioned (see text). Ionic strength (*I*) was adjusted with NaClO₄.

The stock solution of NaClO₄ was prepared by mixing standardized solution of NaOH with the standardized solution of HClO₄. The pH of stock NaClO₄ was adjusted to 6. The concentration of NaClO₄ was further checked by alkalimetry after exchanging a known volume of its dilute solution with Dowex 50W X-8 (H⁺ form) resin and titrating the liberated acid against standard alkali. D₂O was received from Bhaba Atomic Research Centre, India.

2.2 Instrumentation

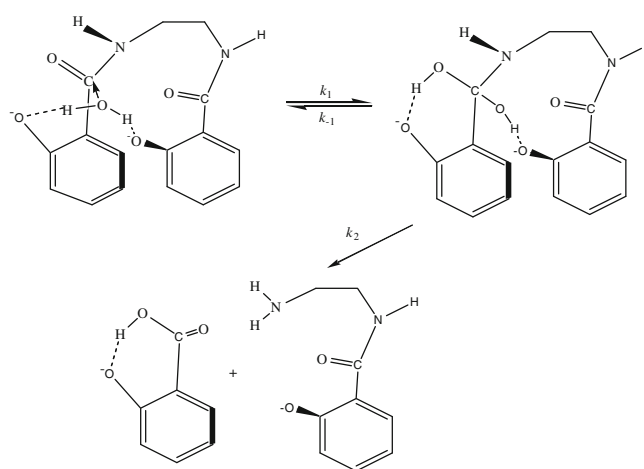
UV-visible absorption spectra and kinetics were monitored with a Cecil spectrophotometer model CE 7200 (U.K.). The cell block was thermostatted to the desired temperature by a thermostatic controller model CE 2024. A pair of 10 mm matched quartz cells was used. The IR spectra were run on a Perkin Elmer 1760X FTIR as KBr pellet. ¹H and ¹³C NMR were recorded on Bruker 400 and 100 MHz NMR spectrometers respectively at IIT Madras. A Systronics pH meter model 335

with glass - Ag/AgCl, NaCl (3 mol dm⁻³) combined electrode CL51 was used for pH measurements.

2.3 Kinetic measurements

The rate measurements were made under pseudo first order conditions at 29.5 ≤ *t*(°C) ≤ 70.0. The reaction mixture containing the desired amounts of all components except the amide was equilibrated in a measuring flask (25 cm³) at the desired temperature in a thermostatic bath. After thermal equilibrium was reached a known volume (2.5 cm³) of methanolic solution of the substrate was quickly transferred to the reaction mixture which was shaken well and transferred to one of the 10 mm quartz cells housed in the thermostatted cell compartment of the spectrophotometer. The progress of the reaction was monitored by the decrease of absorbance at 329 nm measured against solvent blank. The concentrations of the amides were ~ (4–5) × 10⁻⁵ mol dm⁻³ and that of NaOH was varied in the range of 0.02–0.5 mol dm⁻³.

A constant value of absorbance could not be achieved even after 3 days. However, independent measurements (by mixing the corresponding amines, salicylic acid and NaOH, *I* = 0.5 mol dm⁻³) showed that a reaction mixture for the complete hydrolysis of the amides (**I–IV**) to the corresponding amines and salicylate had very small absorbance at the experimental wave length (329 nm). This indicated that the base hydrolysis occurred in two phases, the second one being extremely slow. We, therefore, investigated the first phase of the reaction in which only one amide bond was hydrolysed resulting in the formation of one mole of salicylate per mole of the amides (**I–IV**) hydrolysed. The absorbance time data



Scheme 1. Intra molecular general base catalysed hydrolysis of **I**.

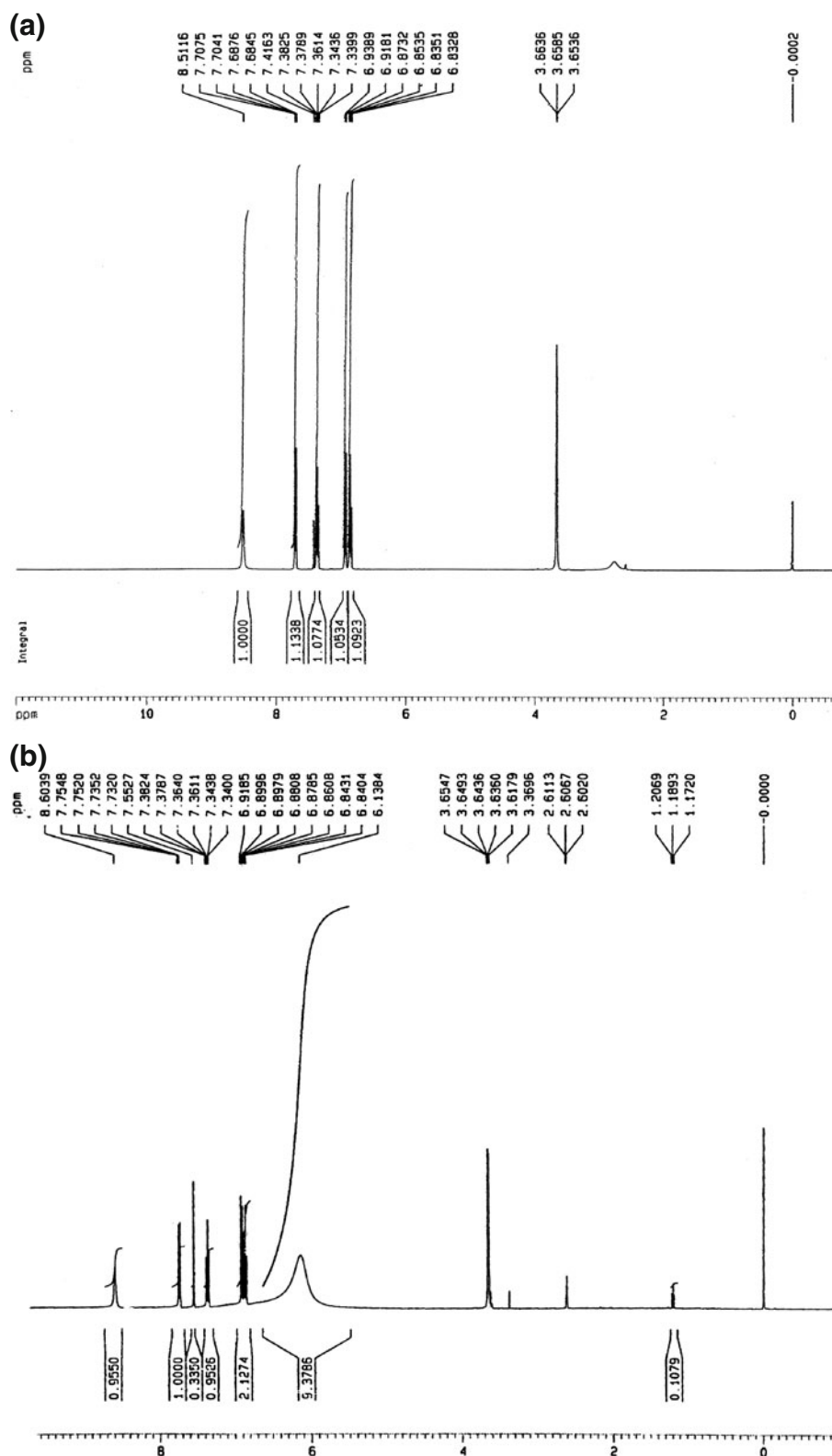


Figure 1. (a) ¹H NMR spectrum of (1,2)bis(2-hydroxyenzamide)ethane (**I**) in (CD₃)₂SO, (b) ¹H NMR spectrum of the hydrolysis product of (**I**) in CDCl₃, (c) ¹³C NMR spectrum of (**I**) in (CD₃)₂SO, (d) ¹³C NMR spectrum of the hydrolysis product of (**I**) in (CD₃)₂SO.

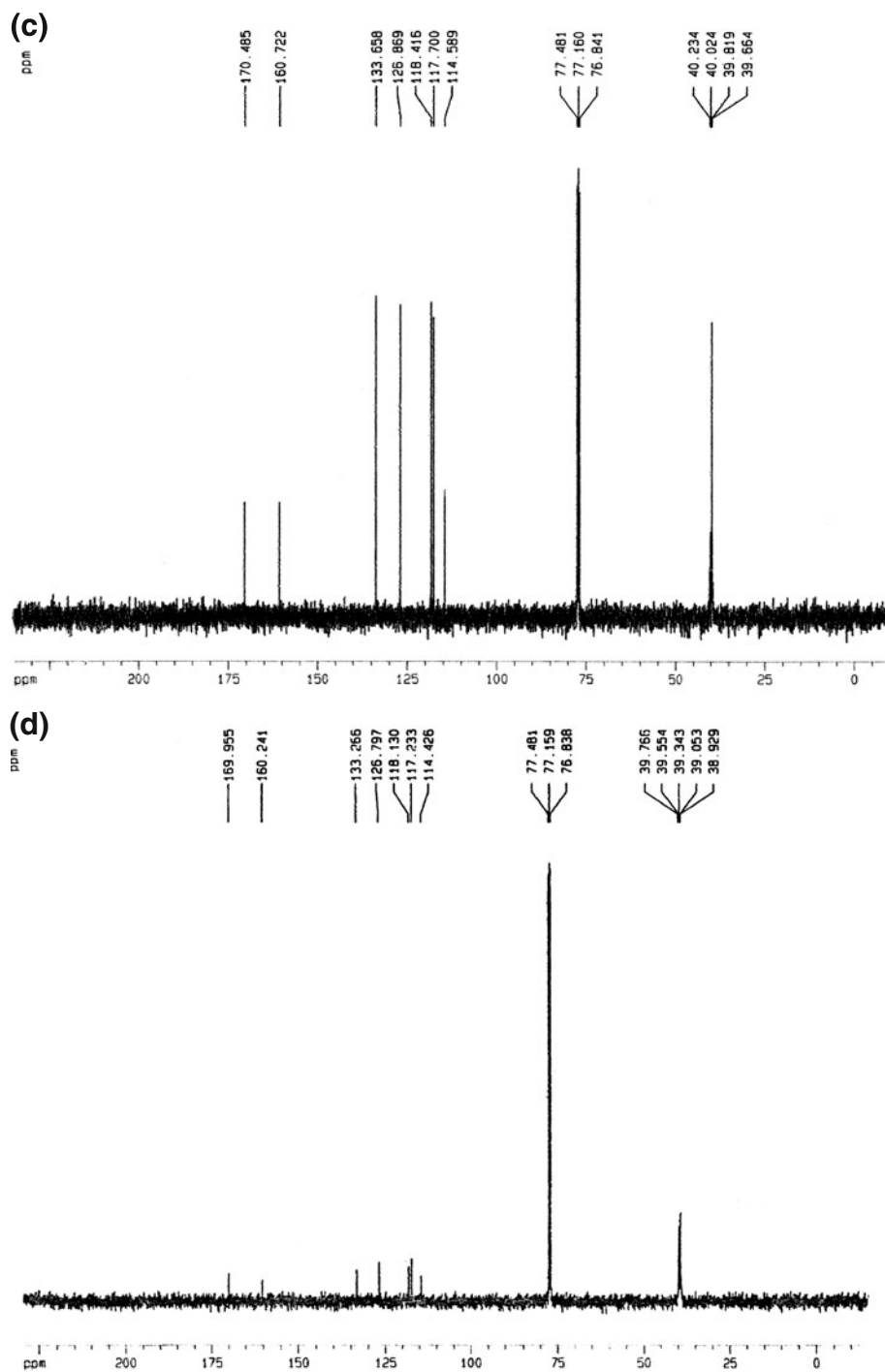


Figure 1. (continued.)

were treated by Guggenheim method¹³ (see equation 1) as the infinity absorbance for the first phase of the reaction was uncertain.

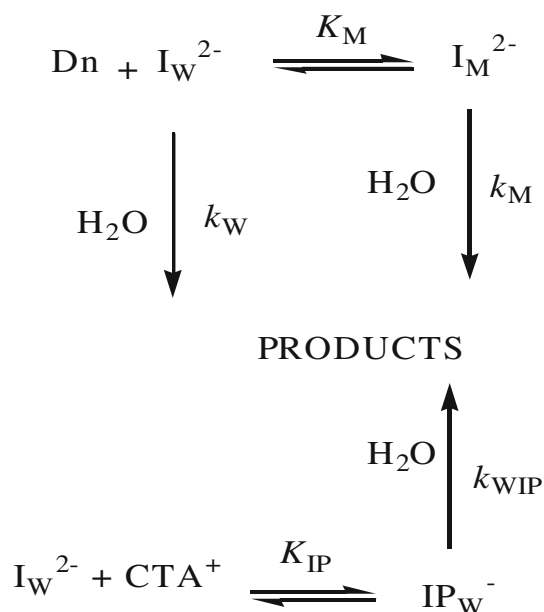
$$A_t - A_{t+\Delta} = C \exp(-k_{\text{obs}}t). \quad (1)$$

In equation (1), $C = (A_0 - A_\infty)\{1 - \exp(-k_{\text{obs}}\Delta)\}$, Δ = a constant time interval and A_t is absorbance at time t . C and k_{obs} were varied and the absorbance-time data

were fitted to equation (1) by a nonlinear least squares program keeping Δ close to *ca.* $t_{1/2}$. The representative absorbance-time plots are shown in figure S1.

2.4 Product analysis

In a typical experiment an aqueous methanolic solution of **I** (0.153 g) was treated with excess of NaOH



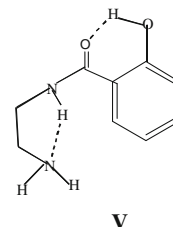
Scheme 2. Hydrolysis of **I** in the presence of CTABr; I_W^{2-} and I_M^{2-} denote $(\text{I}-2\text{H})^{2-}$ in aqueous and micellar pseudo phases respectively.

(0.05 mol dm^{-3}) and the mixture was left for 24 h (*ca.* $\sim 9t_{1/2}$) at room temperature (30°C). The mixture was then acidified with HClO_4 to pH 1 and extracted with CHCl_3 at least thrice. All the CHCl_3 extracts were combined and evaporated to dryness. A white solid was obtained which was dissolved in 0.1 mol dm^{-3} NaOH. After proper dilution in 0.1 mol dm^{-3} alkali the UV spectrum of the solution was recorded and matched with that of salicylic acid under similar condition. Agreement was excellent indicating that the product was salicylic acid. Using a calibration curve of the absorbance of salicylic acid in 0.1 mol dm^{-3} NaOH ($\lambda = 300 \text{ nm}$) it was found that $99 \pm 1\%$ of one of the $-\text{CO}-\text{NH}$ -groups in **I** was hydrolysed yielding salicylic acid. The acidified aqueous extract containing the intermediate displayed characteristic UV spectrum $\{\lambda, \text{nm}(\text{shoulder}) = 300, \lambda_{\text{max}}, \text{nm} = 329\}$ thus confirming that one of the salicylate moiety is present in the intermediate. Similar observations were made for **II-IV**.

In another set of experiment **I** was hydrolysed at 40°C in alkaline medium as described above for 4 h (*ca.* $\sim 4t_{1/2}$), the reaction mixture was then neutralised with dilute HClO_4 and extracted repeatedly with CHCl_3 . The solid obtained by evaporation of the CHCl_3 extract was analysed by ^1H and ^{13}C NMR; the ^1H and ^{13}C NMR spectra of **I** are also presented for comparison (see figures 1a–d).

The product displays a ^1H peak (broad) at 6.136 ppm which does not appear in the ^1H spectrum of **I** and is

thus ascribed to the primary amine function generated during hydrolysis of one of the amide groups; the presence of the other amide group is indicated by the signal at 8.603 ppm corresponding to the same at 8.511 ppm for **I**, a down field shift of 0.092 ppm may be a consequence of the hydrogen bonding of the amide proton with the primary amine site (see Structure **V**).



Further the aliphatic proton signals (3.65–3.66 pp) for **I** are considerably shifted up field (2.602–2.611 ppm) and the spectra become more complex in the aromatic region (7.34–7.754 ppm) upon hydrolysis of one of the amide functions. The ^{13}C NMR spectra (figures 1c, d) also display small shifts of ^{13}C signals on hydrolysis of **I**, the most significant being that of the phenol ($\text{C}-\text{OH}$) and amide ($\text{C}=\text{O}$) functions (160.72, 170.48 ppm for **I**; 160.24 and 169.95 for the hydrolysed product).

3. Results

3.1 Preliminary observations

The repetitive spectral scans for **I-IV** in acidic medium ($[\text{HClO}_4] = 0.05 \text{ mol dm}^{-3}$, 40°C) did not show any change over an extended period thus indicating that the substrates were very stable to acid catalysed hydrolysis. However, they underwent slow base catalysed hydrolysis; clean isosbestic points were observed at 308 nm and 265 nm for **I** and **II** respectively (see figure 2 and inset) during the early phase of the reaction corresponding to the hydrolysis of one amide function.

For **III** and **IV** the isosbestic points appearing around 260, 305 nm and 258, 342 nm respectively were not so well defined during the period of measurement (figure S2 and inset) presumably due to slowness of the reaction. The rate data are collected in table 1. A comparison of the rate and activation parameters is presented in table 2.

3.2 Effect of cetyltrimethylammonium bromide (CTABr)

Rate measurements were made in the presence of the surfactant CTABr for **I** as a representative case to shed

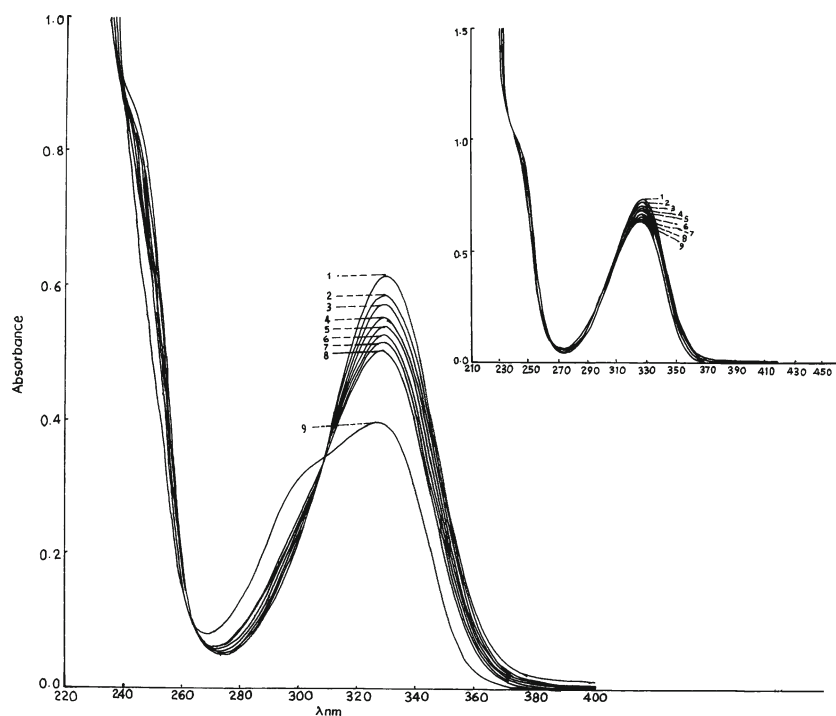


Figure 2. Repetitive spectral scans for the hydrolysis of **I** and **II** (inset) in alkaline medium: 10% MeOH + H₂O (v/v), [NaOH]_T = 0.05, **I** = 0.5 mol dm⁻³; 40°C: 10⁵ [I]_T([II]_T) = 4.80 (6.98) mol dm⁻³, Δ*t* = 15 min (1–8), and 48 h (9); absorbance decreased with time at 329 nm.

light on the mechanism of the reaction (see later). The relevant rate data are collected in table 3. It is interesting to note that there is a substantial retarding effect of the surfactant. The variation of [OH⁻] in the presence of the surfactant had practically no effect on *k*_{obs}.

3.3 Effect of ionic strength

The effect of ionic strength on *k*_{obs} at a constant [OH⁻]_T (= 0.035 mol dm⁻³) was investigated for the representative amide, **I**. We obtained 10⁴*k*_{obs}(s⁻¹) as 0.89 ± 0.06, 0.84 ± 0.02, 0.86 ± 0.02 and 0.88 ± 0.04 at ionic strengths, **I** = 0.05, 0.10, 0.20 and 0.50 mol dm⁻³ (30.5°C) respectively. Thus the observed rate constant is insensitive to the ionic strength variation.

3.4 Solvent isotope effect

The solvent kinetic isotope effect (SKIE) was investigated for **I** in 20% D₂O + 79% H₂O + 1% MeOH (v/v) and 50% D₂O + 49% H₂O + 1% MeOH (v/v) ([OH⁻]_T = 0.035 mol dm⁻³, 40°C) and we obtained *k*_{obs}^{H₂O}/*k*_{obs}^(D₂O+H₂O) as 0.90 ± 0.07 and 1.06 ± 0.02 respectively. As against this substantial slowing down of the

reaction was, however, observed (figure S3) when the proportion of D₂O was raised to 99% (1% MeOH, [OH⁻]_T = 0.02 mol dm⁻³, 40°C) which was attributed to the incomplete ionization of the phenol groups under this condition.

4. Discussion

For all the di-amides (**I–IV**) the second step of hydrolysis was significantly slower than the first one. The rate constant (*k*_{obs}) for the first step was also virtually independent of [OH⁻] (see table 1) once both the phenol groups are completely deprotonated to the phenoxide form. Our earlier data (p*K*_{OH1} and p*K*_{OH2}) of these diphenol diamides showed that these will exist in the *bis* phenoxide form at [OH⁻] ≥ 0.02 mol dm⁻³).^{9,10,14,15} The zero time uv-vis spectral data for **I** at [OH⁻]_T = 0.02 – 0.5 mol dm⁻³ (29°C, **I** = 0.5 mol dm⁻³, 10% MeOH + H₂O) was also independent of [OH⁻] thus supporting that ionization of the phenol groups were complete and further ionization of the amide function(s) of the *bis* phenoxide species did not occur to a measurable extent. The lack of [OH⁻], and ionic strength dependence of *k*_{obs} clearly discounts the possibility of the reaction of the *bis*-phenoxide species with

Table 1. Rate constants for the first step of hydrolysis of the phenol–amide compounds, **I–IV**.^a

[NaOH] (mol dm ⁻³)	10 ⁴ k _{obs} (s ⁻¹) ^b				
	29.5°	35.0°	40.0°	45.0°	50.0°C
I					
0.01	-	-	-	3.20 ± 0.30	
0.02	0.55 ± 0.07	1.02 ± 0.04	1.50 ± 0.03	1.77 ± 0.06 ^d	
0.03	-	0.89 ± 0.17 ^c	1.77 ± 0.04	1.83 ± 0.17 ^d	
0.035	0.72 ± 0.06	-	-	-	
0.04	0.74 ± 0.09 ^d	-	-	-	
0.05	-	1.30 ± 0.02	1.92 ± 0.03	2.20 ± 0.06	
0.10	-	1.51 ± 0.02	1.60 ± 0.15 ^d	1.72 ± 0.04	
0.20	0.81 ± 0.10 ^d	-	-	-	
0.30	-	1.26 ± 0.09	1.63 ± 0.21 ^c	2.03 ± 0.03	
0.50	0.70 ± 0.08	1.45 ± 0.03	1.61 ± 0.30 ^c	2.43 ± 0.06 ^c	
II					
0.01	-	-	2.49 ± 0.12	-	-
0.02	-	-	2.92 ± 0.16	-	-
0.03	-	-	2.63 ± 0.04	-	-
0.05	-	-	2.36 ± 0.10	2.30 ± 0.03	2.40 ± 0.08
0.10	-	-	2.39 ± 0.16	2.75 ± 0.03	3.02 ± 0.05
0.20	-	-	1.96 ± 0.37 ^d	1.78 ± 0.04	2.75 ± 0.03
0.30	-	-	2.88 ± 0.12	2.68 ± 0.03	2.81 ± 0.04
0.40	-	-	2.84 ± 0.31 ^d	2.59 ± 0.06	3.13 ± 0.05
0.50	-	-	1.46 ± 0.03	-	-

^a10% MeOH + H₂O (v/v), Ionic strength (*I*) = 0.5 mol dm⁻³.

^bweighted average of 10⁴k_{obs} (s⁻¹): 0.87 ± 0.05(60.0°C), 1.10 ± 0.35 (65.0°C), 1.68 ± 0.24 (70°C) for **III**, and 1.29 ± 0.31(60.0°C), 1.56 ± 0.09 (65.0°C), 2.25 ± 0.06 (70.0°C) for **IV** at [NaOH]_T = 0.05 and 0.5 mol dm⁻³; w = 1/[σ(k_{obs})]².

^{c,d} weighted average of triplicate (*c*) or duplicate (*d*) runs. All other k_{obs} (and σ(k_{obs})) are from a single run at each [NaOH].

OH⁻. In contrast to these observations Ahmad *et al.*⁸ showed that the phenoxide form of salicylamide underwent base hydrolysis exclusively via [OH⁻] dependent path; the ionization of the amide group of the phenoxide form of salicylamide was detected by them kinetically at an elevated temperature and much higher [OH⁻]_T (= 0.5 – 3 mol dm⁻³, 95°C). In our case deprotonation of the amides is insignificant and also the reactivity of the bis-phenoxide moieties with OH⁻ is negligible which may be ascribed at least partly to the coulombic

repulsion between OH⁻ and the di-negative reactants which does not favour approach of OH⁻ to the reactive HN–C=O centre. The value of k_{obs} at 45°C, [OH⁻]_T = 0.7 mol dm⁻³ (*I* = 3.0 mol dm⁻³) for salicylamide as calculated from the activation parameter data reported by Ahmad *et al.*⁸ turned out 2.5 × 10⁻⁶ s⁻¹. Disregarding the ionic strength effect it turns out that the bis phenoxide form of **I** reacts 80 times faster than the phenoxide form of salicylamide (k_{obs}^I/k_{obs}^{salicylamide} = 80) at the same temperature without being further assisted

Table 2. Comparison of the rate constants and activation parameters.

Compound	10 ⁴ k(25°C)/s ⁻¹ ^{a,b}	ΔH [‡] /kJ mol ⁻¹	ΔS [‡] /J K ⁻¹ mol ⁻¹
I	0.58	49.9 ± 11.1	-(1.58 ± 0.36) × 10 ²
II	1.17	25.7 ± 2.7	-(2.34 ± 0.08) × 10 ²
III	0.064	58.8 ± 3.8	-(1.47 ± 0.11) × 10 ²
IV	0.063	64.8 ± 7.0	-(1.27 ± 0.20) × 10 ²

^acalcd: k = (k_bT/h) × exp(-ΔH[‡]/RT + ΔS[‡]/R).

^bValues of 10⁴k/s⁻¹: 0.69 ± 0.042 (29.5°), 1.37 ± 0.067 (35.0°), 1.72 ± 0.083 (40.0°), 2.00 ± 0.10 (45.0°C) [for **I**]; 1.99 ± 0.20 (40.0°), 2.46 ± 0.17 (45.0°), 2.84 ± 0.09 (50.0°C) [for **II**]; these are the weighted averages of k_{obs} at different [NaOH] (see table 1). For **III** and **IV**, see foot note *b* of table 1.

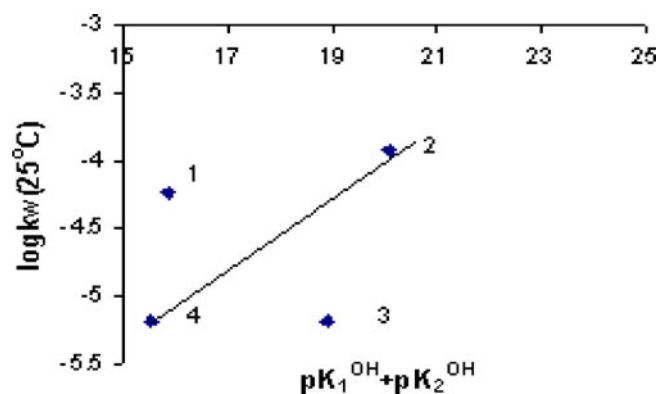


Figure 3. Plot of $\log k_w$ ($25^\circ C$) versus $pK_{1OH} + pK_{2OH}$ for **I**(1), **II**(2), **III**(3) and **IV** (4).

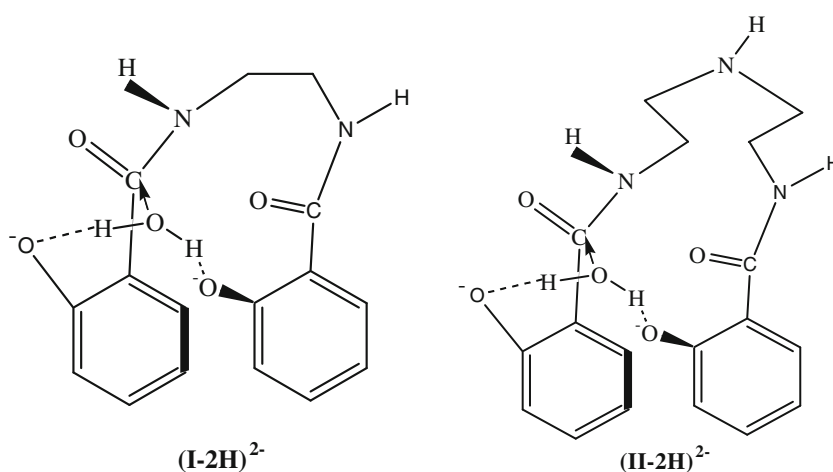


Figure 4. Phenoxide promoted hydration of the amide function.

by $[OH^-]$. This is clearly an indication of the intra molecular general base catalysis of the phenoxide functions on the hydrolysis of the amide bond. However, the reactivity sequence **I** \sim **II** $>$ **III** \sim **IV** (see table 2 and figure 3) further suggests that favourable orientation of the phenoxide moieties with respect to the amide carbonyl function is important for their general base catalytic effect in the attack of H_2O at the $-C=O-NH$ function. When we constructed molecular models of the *bis* phenoxide forms of **I-IV** we found that only for **I** and **II** the two phenoxide groups can be brought close to each other and also proximate to one of the amide carbonyl with a bridging H_2O molecule (see figure 4).

For the other two (**III**, **IV**) the two phenoxide moieties are disposed around the reactive amide function at a longer distance. As such the bridging of the two phenoxide groups through hydrogen bonding necessitates involvement of more water molecules. Consequently the phenoxide promoted hydration of the reactive carbon centre becomes less efficient in the latter case which results in a weaker catalysis. This work,

therefore, clearly delineates the proximity effect on the intra molecular base catalysed hydrolysis of the amide function, a basic unit of considerable importance in macromolecules of biological significance.

A general scheme for the phenoxide catalysed hydrolysis reaction consistent with our observations is presented for **I** in scheme 1. However, the relatively lower reactivities for **III** and **IV** is reconciled with inefficient catalysis of the phenoxide groups due to their larger distance of separation from the reactive $HN-C=O$ centre and also possible involvement of more than one water molecules bridging the phenoxide groups, one of them being an attacking nucleophile.

Consistent with this scheme k_{obs} is given by

$$k_{obs} = k_1 k_2 / (k_{-1} + k_2) \quad (2)$$

Interestingly the observed solvent kinetic isotope effect (SKIE) for **I**, ($k_{obs}^{H_2O} / k_{obs}^{(D_2O+H_2O)} \sim 1$, see above) is comparable in magnitude to the SKIE for the second order base catalysed hydrolysis of *N,N* dimethyl benzamide (0.90 ± 0.18) and *N,N* (ethyl)(1,1,1 trifluoroethyl)

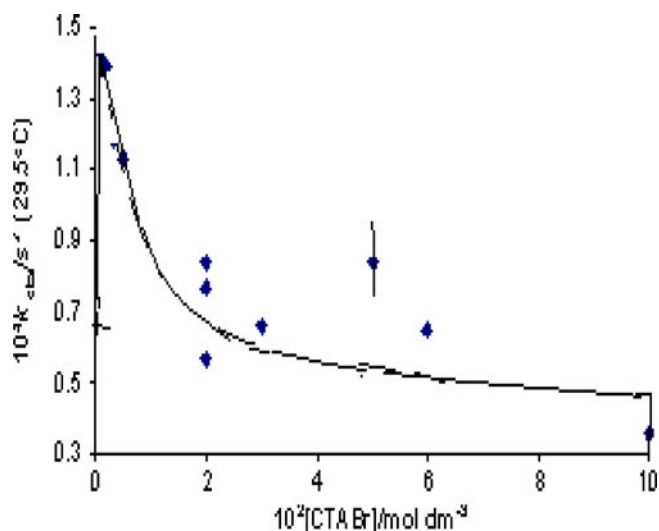


Figure 5. $10^4 k_{\text{obs}}(\text{s}^{-1})$ versus $10^2[\text{CTABr}](\text{mol dm}^{-3})$ plot at 29.5°C . The curve is drawn through $10^4 k_{\text{cal}}(\text{s}^{-1})$ (see table 3) as against the experimental points.

benzamide (1.05 ± 0.04) involving rate limiting nucleophilic addition of OH^- at the amide carbonyl centre.^{1,16} This leads us to believe that proton transfer is not involved in the rate limiting step. The rate determining process essentially involves the nucleophilic attack of H_2O at the amide $\text{C}=\text{O}$ centre (see scheme 1) so that $k_{\text{obs}} \approx k_1 (k_2 > k_{-1})$. This is also in conformity with the recent theoretical calculations on the base hydrolysis of amides in water in which the nucleophilic attack of OH^- at the amide carbonyl function is shown to be the rate determining step.¹⁷

The large negative values of ΔS^\ddagger (see table 2) are consistent with an ordered structure of the transition state as demanded in the k_1 path. However, a relatively larger values of ΔH^\ddagger for **III** and **IV** are in tune with the energy involved in assembling a number of water molecules and bridging the phenoxide moieties for favourably directing the nucleophile to the $\text{C}=\text{O}$ centres for these substrates.

Khan and Azri¹⁸ recently reported that the hydrolysis of the phenoxide form of N-(2'-hydroxyphenyl)phthalimide is retarded by the cationic micelle of CTABr; in this case the reaction involves phenoxide promoted H_2O addition to the $-\text{N}-\text{C}=\text{O}$ moiety (intramolecular general base mechanism). Our observation is similar to that of Khan *et al.*¹⁸ Thus the observed inhibitory effect of CTABr (see figure 5) on the rate of hydrolysis of the dianion of **I**, $(\text{I}-2\text{H})^{2-}$ is consistent with the absence of the OH^- dependent path, the reaction being mediated by the general base catalytic effect of the phenoxide groups favourably

disposed around the reaction centre and directing a molecule of water to the amide $\text{C}=\text{O}$ centre.

Figure 5 further depicts that there is a catalytic effect of CTABr at $<0.001 \text{ mol dm}^{-3}$. This, we believe, is due to the influence of a pre-micellar aggregate. Considering the coulombic interaction between CTA^+ and the reactant, $(\text{I}-2\text{H})^{2-}$, the pre-micellar aggregate may be an ion-pair.

On the basis of the pseudo phase (PP) model¹⁹ and including reactive ion-pair formation in the aqueous pseudo phase, scheme 2 is proposed.

Accordingly, the observed rate constant is given by equation (3).

$$k_{\text{obs}} = \frac{k_{\text{W}} + k_{\text{WIP}}K_{\text{IP}}[\text{CTA}^+] + k_{\text{M}}K_{\text{M}}[\text{Dn}]}{1 + K_{\text{IP}}[\text{CTA}^+] + K_{\text{M}}[\text{Dn}]} \quad (3)$$

Using $[\text{CTA}^+] = \text{c.m.c.}$, $[\text{Dn}] = [\text{CTABr}]_{\text{T}} - \text{c.m.c.}$, $K'_{\text{M}} = K_{\text{M}}/(1 + K_{\text{IP}}[\text{CTA}^+])$, $k'_{\text{W}} = (k_{\text{W}} + k_{\text{WIP}}K_{\text{IP}}[\text{CTA}^+])/(1 + K_{\text{IP}}[\text{CTA}^+])$, equation (3) is recast as equation (4).

$$k_{\text{obs}} = (k'_{\text{W}} + k_{\text{M}}K'_{\text{M}}[\text{Dn}]) / (1 + K'_{\text{M}}[\text{Dn}]) \quad (4)$$

A weighted least squares²⁰ fit to the linearized form of equation (4), using $1.45 \leq 10^4 k'_{\text{W}}(\text{s}^{-1}) \leq 1.70$, and $0.3 \leq 10^4 \text{ c. m. c.} \leq 4.0 \{ (k'_{\text{W}} - k_{\text{obs}})^{-1} \text{ versus } [\text{Dn}]^{-1} \text{ plot} \}$, yielded the first approximate values of $k_{\text{M}}K'_{\text{M}}$ and K'_{M} ; the best fit values (corr. coeff. = 0.9802) of K'_{M} and $10^4 k_{\text{M}}$ were $121 \pm 21 \text{ dm}^3 \text{ mol}^{-1}$ and $0.29 \pm 0.14 \text{ s}^{-1}$

Table 3. Effect of CTABr on hydrolysis of **I**.^a

$[\text{OH}^-]_{\text{T}}$ (mol dm^{-3})	$[\text{CTABr}]_{\text{T}}$ (mol dm^{-3})	$10^4 k_{\text{obs}}$ (s^{-1})	$10^4 k_{\text{cal}}^{\text{c}}$ (s^{-1})
0.05	0.0010	1.43 ± 0.03	1.46
0.05	0.0020	1.39 ± 0.04	1.32
0.05	0.0050	1.13 ± 0.07	1.05
0.05	0.010	0.85 ± 0.01	0.84
0.05	0.030	0.66 ± 0.04	0.60
0.05	0.050	$0.84 \pm 0.11^{\text{b}}$	0.54
0.05	0.060	0.65 ± 0.05	0.52
0.05	0.100	$0.36 \pm 0.11^{\text{b}}$	0.48
0.01	0.020	0.77 ± 0.02	0.67
0.02	0.020	0.84 ± 0.04	0.67
0.03	0.020	0.57 ± 0.02	0.67
0.04	0.020	0.57 ± 0.02	0.67

^a $29.5 \pm 0.1^\circ\text{C}$; $[\text{I}]_{\text{T}}: (2.8-5.5) \times 10^{-5} \text{ mol dm}^{-3}$; 10%(v/v)MeOH + H_2O medium.

^bAverage of duplicate runs; all other $k_{\text{obs}}(\pm\sigma_{k_{\text{obs}}})$ values are from a single run for a given condition.

^cSee equation (4): $10^4 k_{\text{W}}' = 1.66 \pm 0.16 \text{ s}^{-1}$, $10^4 k_{\text{M}}K'_{\text{M}} = 79.1 \pm 56.0 \text{ dm}^3 \text{ mol}^{-1} \text{ s}^{-1}$, $K'_{\text{M}} = (1.90 \pm 0.87) \times 10^2 \text{ dm}^3 \text{ mol}^{-1}$, $\sum [(k_{\text{cal}} - k_{\text{obs}})/\sigma_{k_{\text{obs}}}]^2 = 118.7$, c. m. c. = $1.0 \times 10^{-4} \text{ mol dm}^{-3}$.

respectively with $10^4 k'_w (s^{-1}) = 1.50$ and 10^4 c. m. c. = 1.0 mol dm^{-3} . The value of c. m. c. was then held fixed at $1.0 \times 10^{-4} \text{ mol dm}^{-3}$, the k_{obs} data were refitted to equation (4) by a weighted nonlinear least squares computer program using the first approximate values of k'_w , $k_M K'_M$ and K'_M . We obtained $10^4 k'_w (s^{-1}) = 1.66 \pm 0.16$, $10^4 k_M K'_M (\text{dm}^3 \text{ mol}^{-1} \text{ s}^{-1}) = 79.1 \pm 56.0$ and $10^{-2} K'_M (\text{dm}^3 \text{ mol}^{-1}) = 1.90 \pm 0.87$ which gave $10^4 k_M (s^{-1})$ as 0.42 ± 0.35 (see foot note *c* of table 3). It is thus evident that the micellar binding of $(\text{I}-2\text{H})^{2-}$ reduces its reactivity ($10^4 k_w (s^{-1}) = 0.69 \pm 0.04$) despite the fact that the residence site of this reactive dianion is predominantly the water-rich region of the micellar pseudo phase. Our result is consistent with the earlier observations that the decreased availability of water in the micellar pseudo phase as also its lower polarity than bulk water, slow down the water addition reactions.^{19(a), 21}

Now turning to the value of k'_w a reasonable assessment of the reactivity of the IP can be made as follows. If it is assumed that $K_{\text{IP}} [\text{CTA}^+] ([\text{CTA}^+] = \text{c. m. c.}) \ll 1$ and $K_{\text{IP}} < 10^3 \text{ dm}^3 \text{ mol}^{-1}$ then $k_{\text{WIP}} \{=(k'_w - k_w)/[\text{CTA}^+], [\text{CTA}^+] = 1.0 \times 10^{-4} \text{ mol dm}^{-3}\}$ assumes a value $>(1.0 \pm 0.2) \times 10^{-3} \text{ s}^{-1}$ (29.5°C, using $k_w = 0.69 \pm 0.045 \times 10^{-4} \text{ s}^{-1}$, see foot note *c* of table 2). A substantial catalytic effect of the ion-pair ($k_{\text{WIP}}/k_w > 14 \pm 3$) in the aqueous pseudo-phase is envisaged. On the other hand, if $K_{\text{IP}} \sim 10^5 \text{ dm}^3 \text{ mol}^{-1}$ then k_{WIP} turns out $1.6 \pm 0.2 \times 10^{-4} \text{ s}^{-1}$; the ion-pair only nominally catalyses the reaction ($k_{\text{WIP}}/k_w = 2.3 \pm 0.3$). The

ion-pair formation constant for 2-, +1 charge type interaction in aqueous medium is predicated from the coulombic concept to be $<10 \text{ dm}^3 \text{ mol}^{-1}$ for the hard sphere ions.²² In this particular case it is hard to believe that K_{IP} value will exceed 10^3 . The value of K'_M negates such a possibility also. Hence we prefer the former interpretation. A relatively high value of K_{IP} ($\sim 10^3$) for the interaction between CTA^+ and $(\text{I}-2\text{H})^{2-}$ in aqueous environment is likely to be due to both coulombic and hydrophobic effects (see figure 6), the latter possibly squeezes the reactive anion favourably due to coiling of the tail of the surfactant ion and accelerates the water addition at the C=O function.

The rate acceleration due to this kind of capping effect was earlier observed by us in the intra molecular isomerization of O-bonded sulphite to its S-bonded form in the case of (tetren)Co-OSO₂⁺ when the reaction was carried out in the presence of sodium dodecyl sulphate (SDS).²³

5. Conclusion

The present work demonstrates that the *bis* phenoxide species of (1,2)*bis*(2-hydroxybenzamido)ethane (I), (1,5)*bis*(2-hydroxybenzamido)3-azapentane (II), (1,3)*bis*(2-hydroxybenzamido)propane (III), and (1,8)*bis*(2-hydroxybenzamido)3,6-diazaoctane (IV) undergo exclusively phenoxide promoted hydrolysis

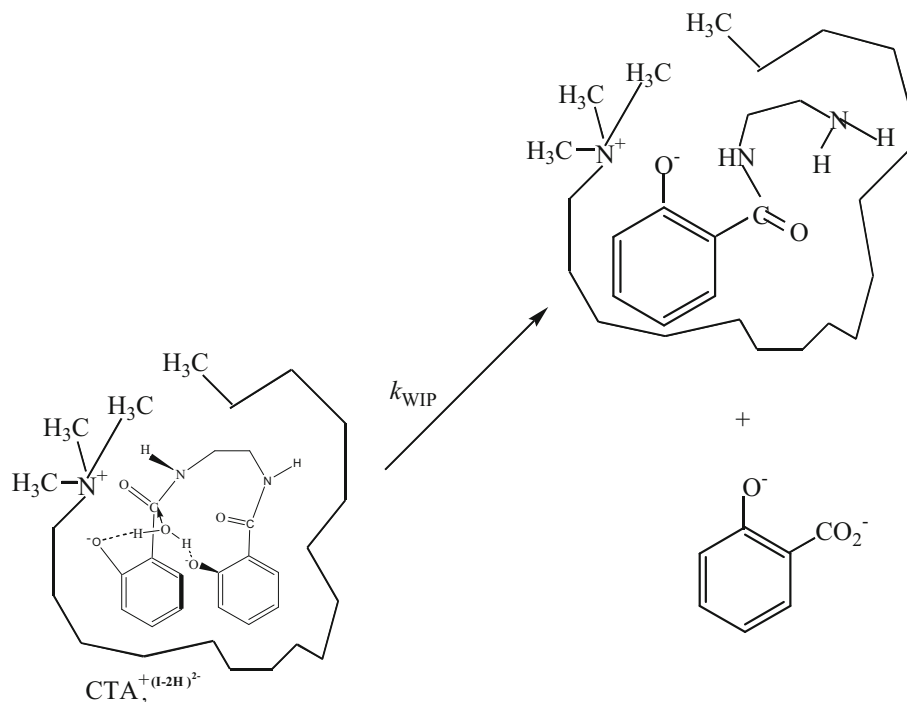


Figure 6. Tentative structure of the ion-pair, $\text{CTA}^+, (\text{I}-2\text{H})^{2-}$ and its reaction.

(general base catalysis) of one of the amide bonds. The observed reactivity trend: **I** ~ **II** >> **III** ~ **IV** depicts the proximity effect of the two phenoxide moieties in the same molecule in the rate limiting hydration of the amide carbonyl function. This is supported by the low values of the activation enthalpy $\{\Delta H^\ddagger$ (kJ mol⁻¹): 49.9 ± 11.1 (**I**), 25.7 ± 2.8 (**II**), 58.8 ± 3.8 (**III**), and 64.8 ± 7.0 (**IV**)}. The substantially low values of ΔS^\ddagger $\{-158 \pm 36$ (**I**), -234 ± 8 (**II**), -147 ± 11 (**III**) and -127 ± 20 (**IV**) J K⁻¹ mol⁻¹} are also consistent with closely similar, and ordered transition states which can be assembled by favourably oriented phenoxide groups. The solvent kinetic isotope effect (SKIE), $k^{\text{H}_2\text{O}}/k^{\text{D}_2\text{O}+\text{H}_2\text{O}} \sim 1$ (20 and 50 volume % D₂O) for **I** indicates that proton transfer is not involved as a part of the rate controlling process. The observed slowing down of the rate of this reaction for **I** in the micellar pseudo phase of CTABr also supports the proposed mechanism. Under pre-micellar conditions, however, rate acceleration is observed due to the ion-pair catalysis, a consequence believed to be associated with the capping effect of the hydrophobic tail of the surfactant cation, forming the ion-pair, CTA⁺,(I-2H)²⁻ exclusively in the aqueous pseudo phase.

Acknowledgements

SCD is thankful to the University Grants commission, India for the award of a teacher fellowship, to the Principal and Governing Council of Nimapara College, Nimapara, Orissa, India for granting study leave and to the Head of the Department of Chemistry, Utkal University for extending infrastructural facilities.

Supplementary material

Figure S1 showing the absorbance versus time plots for **I–IV**, Figures S2 (for **II**, **III**) and S3 (for **I**) showing the repetitive spectral scans for the hydrolysis in H₂O + MeOH, and D₂O (90% v/v) are submitted as supplementary material (see www.ias.in/chemsci).

References

1. Brown R S, Bennet A J and Slebocka-Tilk H 1992 *Acc. Chem. Res.* **25** 481
2. Bowden K, Hiscocks S P and Reddy M K 1997 *J. Chem. Soc. Perkin Trans.* **2** 1133
3. Sunatsuki Y, Nakamura M, Matsumoto N and Kai F 1997 *Bull. Chem. Soc. Jpn.* **70** 1851
4. Stassinopoulos A, Schulte G, Papaefthymiou G C and Caradonna J P 1991 *J. Am. Chem. Soc.* **113** 8686
5. Stassinopoulos A and Caradonna J P 1990 *J. Am. Chem. Soc.* **112** 7071
6. Nguyen C, Guarjardo R J and Mascharak P K 1996 *Inorg. Chem.* **35** 6273
7. Nayak S, Dash A C and Lahiri G K 2008 *Transit. Met. Chem.* **33** 39 and references cited therein
8. Ahmad R, Khan M N and Khan A A 1976 *Ind. J. Chem.* **14A** 807
9. Dash A C and Mishra A N 1998 *Ind. J. Chem.* **37A** 961
10. Nayak S and Dash A C 2003 *Ind. J. Chem.* **42A** 2427
11. Dash A C and Rath R K 2004 *Ind. J. Chem.* **43A** 310
12. Chandra S K and Chakravorty A 1992 *Inorg. Chem.* **31** 760
13. Frost A A and Pearson R G 1961 *Kinetics and mechanism*, 2nd edn (New York: Wiley) p 49
14. Nayak S, Dash A C, Nayak P K and Das D 2005 *Transit. Met. Chem.* **30** 917
15. Nayak S and Dash A C 2006 *Transit. Met. Chem.* **31** 813
16. Slebocka-Tilk H, Bennet A J, Keillor J W, Brown R S, Guthrie J P and Jodhan A J 1990 *J. Am. Chem. Soc.* **112** 8507; (b) Slebocka-Tilk H., Bennet A J, Hogg A J and Brown R S 1991 *J. Am. Chem. Soc.* **113** 1288
17. Galabov B, Cheshmedzhieva D, Ilieva S and Hadjieva B 2004 *J. Phys. Chem.* **A108** 1147
18. Khan N and Azri H R 2010 *J. Phys. Chem.* **B 114** 8089
19. Al-Lohedan H, Bunton C A and Mhala M M 1982 *J. Am. Chem. Soc.* **104** 6654; (b) Dash A C, Dash B ad Panda D 1985 *J. Org. Chem.* **50** 2905
20. For $Y = (k'_W - k_{\text{obs}})^{-1}$, $\sigma(Y) = \sigma(k_{\text{obs}}) \times (k'_W - k_{\text{obs}})^{-2}$, and $w(Y) = [\sigma(Y)]^{-2}$
21. Menger F M, Yoshinaga H, Venkatasubban K S ad Das A R 1981 *J. Org. Chem.* **46** 415
22. Fuoss R 1958 *J. Am. Chem. Soc.* **80** 5059; Eigen M 1954 *Z. Physik. Chem. (Frankfurt)* **1** 176
23. Dash A C and Patnaik A K 1995 *J. Chem. Res. (S)* 230 (*M*) 1529